

Stjepan Tvorčić, PhdUniversity of Applied Sciences, Zagreb
Croatia**Miroslav Petrinić, Phd**KONČAR – Electrical Engineering Institute
Croatia**Ante Elez, Phd**KONČAR – Generators and Motors
Croatia**Mario Brčić**KONČAR – Generators and Motors
Croatia

Static eccentricity fault detection method for electrical rotating machines based on the magnetic field analysis in the air gap by measuring coils

SUMMARY

Electrical rotating machines have a great economic significance as they enable conversion of energy between mechanical and electrical state. Reliability and operation safety of these machines can be greatly improved by implementation of continuous condition monitoring and supervisory systems. Especially important feature of such systems is the ability of early fault detection. For this reason, several methods for detection and diagnosis of the machine faults have been developed and designed. As fault detection methods can largely differ in the types of detectable faults, machine adoptability and price of the system, a novel method was developed that can be used for cost-effective detection of various faults of electrical machine. Machine fault detection technique presented in this paper is based on the measurement of magnetic field in the air gap. Numerous studies have proven that crucial information about the machine condition can be determined based on measurement and analysis of the magnetic field in the air gap. It has also been confirmed that analysis of the air gap magnetic field can be used to detect, diagnose and recognize various electrical faults in their very early stage. Proposed method of positioning and installation of the measuring coils on ferromagnetic core parts within the air gap region of the machine enables differentiation of various faults. Furthermore, different faults can be detected if measuring coils are placed on the stator teeth then when placed on the rotor side. The paper presents method on how to analyse and process the measured voltages acquired from measuring coils placed within the machine, especially in the case of rotor static eccentricity detection. The methodology is explained by means of finite element method (FEM) calculations and verified by measurements that were performed on the induction machine. FEM calculation model was used to predict measurement coil output of the induction motor for healthy and various faulty states (at different amounts of static eccentricity). These results were then confirmed by measurements performed in the laboratory on the induction traction motor that was specially modified to enable measurements of faulty operation states of the machine. Measurements comprised of several machine fault conditions broken one rotor bar, broken multiple rotor bars, broken rotor end ring and various levels of rotor static eccentricity.

Other methods used for faults detection are primarily based on the monitoring of quantities such as current and vibration and their harmonic analysis. This new system is based on the tracing the changes of induced voltage of the measuring coils installed on the stator teeth. Faults can be detected and differentiated based on RMS value of these voltages and the number of voltage spikes of voltage waveform i.e. without the need of harmonic analyses. If these coils are installed on the rotor it is possible to detect the stator winding faults in a similar manner.

KEYWORDS

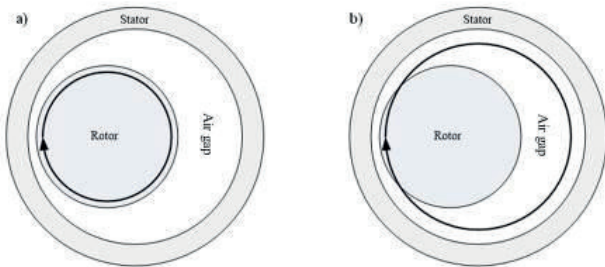
static eccentricity, induction machine, squirrel-cage rotor, finite element, magnetic field, air gap, measuring coil, faults detection

INTRODUCTION

Induction motors are one of the most common types of electrical rotating machines. These machines play an important role independently or as part of a complex process, and are widely present in the power plants, oil refineries, chemical plants, metal foundries, pumping stations, coal mills, paper industry, etc. Because of the importance in the process, it is necessary to prevent failures and ensure reliability and availability of key induction motors. To achieve these tasks all key machines, contain some types of protection, supervision, and monitoring. Also, one of the main goals is early and reliable fault detection and provision of mutual recognition of each fault. Majority of induction motor faults is caused by electrical and mechanical conditions of the machine combined with operational environment. According to the literature [1 – 4], the most common faults of induction machines are bearing faults, following stator and rotor faults and other faults such as different types of eccentricity (static, dynamic or both). In order to early detect and recognize induction machine fault, various types of fault detection methods have been developed [5, 6, 7, 8]. These methods are a result of long-term testing, measurement, and monitoring of the induction machine operation. All these methods with more or less success enable fault detection of induction motor.

One of the common motor problems is the occurrence of rotor static eccentricity that exceeds the allowable limit [9]. There are generally two kinds of rotor eccentricities: static or dynamic (showed on the figure 1). In the case of static eccentricity, the rotor turns around its centre of gravity, but this centre is displaced of the stator centre line. From the stator point of view, the place of minimal air gap occurs at unchanged circular position. In the dynamic eccentricity case, the central axis of the rotor is not fixed but during rotation changes its position relative to the stator centre line. In this case the position of minimal airgap does not stay at the same stator circular position, but rather changes in time. Within this paper only the phenomenon of static eccentricity was analysed. The occurrence of rotor static eccentricity in induction machine can cause some of the following undesirable effects: vibrations, unbalanced magnetic pull (UMP), additional losses in the rotor winding and in parallel circuits of the stator windings, occurrence of the shaft voltages and currents, additional losses in the stator or rotor core, and finally in the worst case scenario physical contact of the rotor with the stator [10]. These undesirable effects either reduce the machine performance and efficiency or make secure operation of the machine impossible and therefore lead to the complete machine shutdown.

Figure 1. Types of eccentricities: a) static b) dynamic



In order to early detect and recognize static eccentricity problem, various types of fault detection methods have been developed [11, 12, 13, 14]. This paper presents new methodology for static eccentricity detection that was developed as part of the continuous research in the field of rotating machine fault detection techniques. The basis for this new innovative methodology can be find in the previous research that was presented within the paper [15]. Within the previous research the squirrel-cage faults (such as broken bar/s or ring) and the possibility of their early fault detection were analysed.

The new approach for rotor static eccentricity detection described in this paper is based on the air-gap magnetic field analysis. Presented methodology is more reliable and requires less data processing than other known methods. The magnetic field is determined by measuring coils embedded in the machine airgap, installed on the stator teeth, and mutually spaced for the pole pitch. Based on the voltage waveforms and RMS values of the induced voltages in the measuring coils it is possible to detect rotor eccentricity of the induction machine. In the paper results obtained by finite element method (FEM) and measurement on the real induction motor are presented. In order to show changes in the induced voltage waveforms and RMS voltage values of the measuring coils, numerical simulations on the FEM model have been performed. At first, FEM calculation for a regular motor operation was conducted. Then, using the same FEM model with modifications in placement of the machine rotor centre point position the cases of static eccentricity were simulated. In the FEM model, the rotor of

the motor was shifted in the direction of $\pm y$ axes for achieving differences in static eccentricity. To detect the existence of static eccentricity, induced voltages in measuring coils mutually spaced for the pole pitch were observed and analysed. Based on the RMS value change of the induced voltage in the coils, the presence of rotor displacement and static eccentricity was determined. FEM result were verified through measurements on the induction machine.

The aim of the paper is a contribution to early and reliable rotor eccentricity detection of induction machines, based on the magnetic field analysis in the air gap. The novelty of this new methodology is magnetic field analysis obtained by measuring coils installed in the airgap of induction machine. The main advantage of this methodology is that it avoids complex signal processing and the need for harmonic analysis of the measured signal. The presence of rotor static eccentricity is determined by detection of changes in induced voltage waveform and RMS value in the measuring coils, mutually spaced for a pole pitch.

FEM ANALYSIS OF THE INDUCTION MACHINE

The FEM analysis was performed in the commercial software *Infolytica Magnet*. Two-dimensional FEM model of the squirrel-cage induction motor is showed on the figure 2.a). The figure 2.b) shows distribution of the magnetic field together with the position of the measuring coils. These measuring coils are in the airgap, installed on the stator teeth and circularly spaced for a pole pitch, p_p . To achieve reliable static eccentricity detection, it is necessary to ensure exactly this kind of measuring coils layout. Based on the waveform and RMS value of the induced voltage in the measuring coils it is possible to detect rotor eccentricity of the induction machine. To determine changes of these voltage values, numerical simulations on the FEM model have been performed. Table 1 lists regular and simulated faulty conditions of the analysed induction motor. Percentage of eccentricity is given in relation to the minimal air gap width. First, FEM calculation for a regular machine operation was performed. Then, using the same model with corresponding modifications the simulations of static eccentricity were performed. In the FEM model, the machine rotor was shifted in the direction of $\pm y$ axes for achieving changes of static eccentricity. The influence on the induced voltage in measuring coils circularly spaced for a pole pitch was observed and analysed with aim to detect the static eccentricity presence. Based on the RMS value change of the induced voltage in the coils, the presence of rotor displacement and static eccentricity is determined.

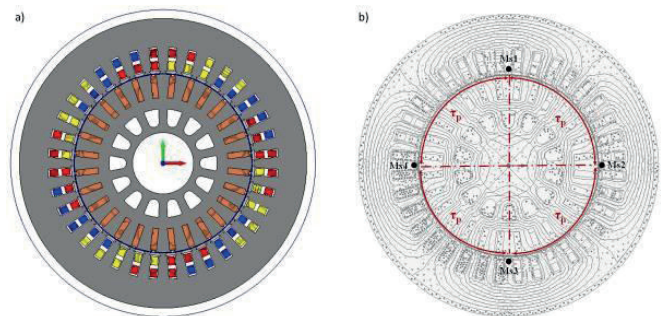


Figure 2. a) 2D FEM model; b) distribution of the magnetic field with position of the measuring coils

Table 1. Calculated regular and faulty conditions of the induction machine

Operating state	Regular condition	Faulty condition – static eccentricity	Model variant
Induction machine rated load	●		-
		●	15 % of static eccentricity
		●	20 % of static eccentricity
			25 % of static eccentricity

The figure 3.a) shows the voltage waveform induced in the measuring coils mutually spaced for the pole pitch, p_p obtained for regular operation condition. For correct voltage waveform interpretation, it is necessary to have certain information regarding machine active part elements and understand their impact on the measuring coil voltage waveform. Figure 3.b) presents the impact of the squirrel-cage rotor bars on the induced voltage waveform in the measuring coils. Numbers on this figure mark the impact

of every rotor bar on the waveform. In one rotor turn, the waveform contains the number of rises and drops of the voltage that is exactly equal to the number of rotor bars. In the analysed case the induction machine has 28 rotor bars.

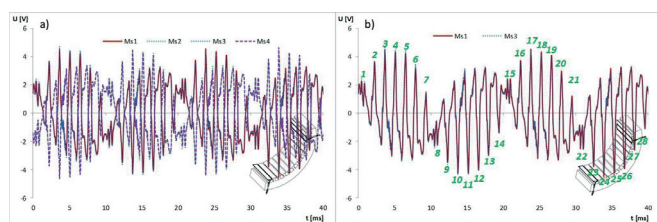


Figure 3. a) Induced voltage waveform in the measuring coils Ms1, Ms2, Ms3 and Ms4 – normal condition; b) impact of the squirrel-cage rotor bars on the induced voltage waveform

Following the regular machine operation, FEM simulations of static eccentricity listed in the table 1 were performed. Figure 4 shows induced voltage waveform in the measuring coils when rotor is displaced for 25 % of the air gap width in the $-y$ axis direction. Figure 4.a) shows comparison of the induced voltage in the measuring coils Ms1 and Ms3, and figure 4.b) comparison of the voltage in the measuring coils Ms2 and Ms4. Through observation of these figures it can be noticed that the absolute value of voltage induced in the coil Ms3 is greater than the voltage induced in the coil Ms1. This result is expected, as the chosen rotor displacement direction places squirrel-cage rotor nearest to the coil Ms3, and farthest apart from the coil Ms1. The comparison of the induced voltage in the measuring coils Ms2 and Ms4 is shown on the figure 4.b). From this figure it can be concluded that the induced voltage in the mentioned measuring coils are equal. This result is expected as, in case of the chosen rotor displacement direction, the relative position of the rotor to these two coils stays the same.

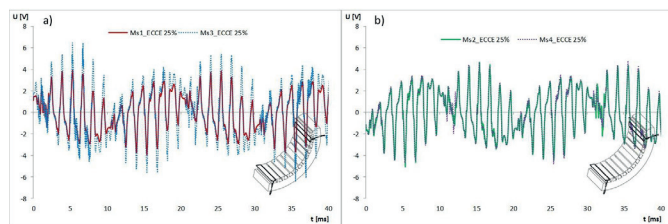


Figure 4. Comparison of the induced voltage waveform in the measuring coils for the static eccentricity amount 25% of the air gap (a shift in the $-y$ axis): a) Ms1 and Ms3 diametrically spaced; b) Ms2 and Ms4 diametrically spaced

RMS values of the induced voltages in the measuring coils Ms1, Ms2, Ms3 and Ms4 obtained by FEM calculations due to the vertical rotor displacement are listed in table 2. These results lead to the following conclusions: when a static eccentricity occurs, induced voltage reaches the highest value in the coil that is nearest to the rotor, and the lowest in the coil that is farthest to the rotor; when the rotor is shifted in $+y$ direction, the highest voltage is induced in the measuring coil Ms1 and the lowest in Ms3; when the rotor is shifted in $-y$ direction, the highest voltage is induced in the measuring coil Ms3 and the lowest in Ms1; induced voltage value changes depending on the static eccentricity amount; the induced voltage values in the measuring coils Ms2 and Ms4 practically stayed unchanged with rotor displacement (positions perpendicular to the displacement direction, where the air gap size stays the same). In the case of the normal condition (without the presence of static eccentricity) the induced voltage values and the waveforms of the four measuring coils are symmetrical. The rotor displacement leads to differences in induced voltage waveforms and the RMS voltage values of the measuring coils. The last column in the table 2 shows the percentage deviation between the measuring coils with the highest voltage change due to the rotor displacement in the vertical direction. Based on the data in the table 2 the dependency curves between the induced voltage in the measuring coils and the rotor displacement in the vertical direction were determined. The figure 5.a) shows changes of the induced voltage RMS values in the measuring coils Ms1 and Ms3 and the figure 5.b) changes of the induced voltage RMS values in the measuring coils Ms2 and Ms4, due to rotor displacement in the vertical direction for different amounts of static eccentricity.

Table 2. RMS values of the induced voltage in the measuring coils obtained by FEM calculations due to the rotor displacement in a vertical direction

Δ [mm]	Motion direction	MS1 [V]	MS2 [V]	MS3 [V]	MS4 [V]	$\Delta U_{MS1/MS3}$ [%]
-0,25	to $-y$	2,155	2,468	3,011	2,533	39,72
-0,20	to $-y$	2,213	2,475	2,894	2,520	30,74
-0,15	to $-y$	2,283	2,484	2,777	2,522	21,66
0,00	centre	2,422	2,422	2,421	2,424	0,00
0,15	to $+y$	2,764	2,505	2,265	2,468	22,06
0,20	to $+y$	2,901	2,525	2,221	2,483	30,58
0,25	to $+y$	3,012	2,535	2,159	2,472	39,52

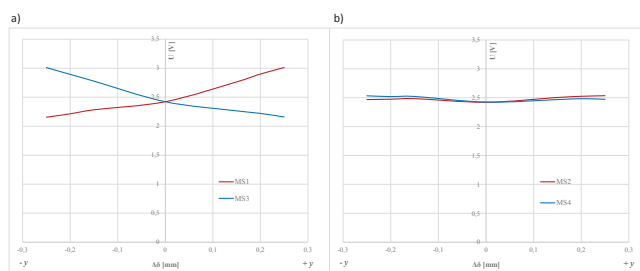
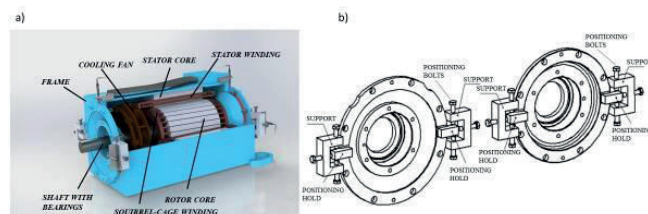


Figure 5. Changes of the induced voltage RMS values in the measuring coils due to rotor displacement in the vertical direction for different amounts of static eccentricity: a) measuring coils Ms1 and Ms3; b) measuring coils Ms2 and Ms4

MEASUREMENTS ON THE INDUCTION MACHINE

The measurements were performed on the squirrel-cage induction machine. The figure 6.a) shows analysed induction machine main parts. This motor was specially modified in order to analyse static eccentricity effects in the laboratory conditions. The eccentricity level control was possible due to the redesign of motor bearing shields, shown on the figure 6.b). The shown mechanism allows the change of rotor static eccentricity position through tightening of the positioning bolts. Figure 7.a) shows the positions of measuring coil installation on the stator teeth of the machine. The position and layout of the measuring coils installed in the tested motor is shown on the figure 7.b). The results obtained by measurements for regular condition are shown on the figure 8. The figure 8.a) shows the induced voltage waveform of the measuring coils Ms1, Ms2, Ms3 and Ms4, and the figure 8.b) the voltage induced in the coils Ms5, Ms6, Ms7 and Ms8.

Figure 6. a) Squirrel-cage induction machine analysed in the laboratory; b) bearing shields adapted for static eccentricity simulation on the machine tested in the laboratory



shields adapted for static eccentricity simulation on the machine tested in the laboratory

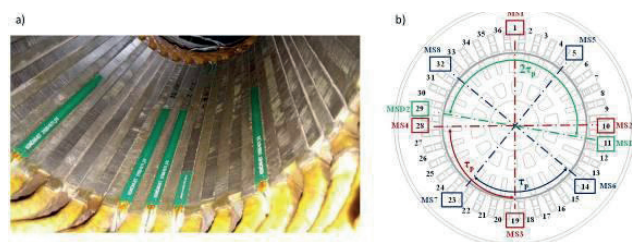


Figure 7. a) Measuring coil installation on the stator teeth of squirrel-cage induction machine; b) position of the measuring coils in the induction machine adapted for laboratory testing

Figure 9 shows results obtained by measurement for the case of 25 % of static eccentricity and the rotor displacement in the $-y$ axis. On the figure 9.a) the voltage waveforms of the measuring coils Ms1 and Ms3 are shown, and on the figure 9.b) induced voltage in the measuring coils Ms2 and Ms4. The result obtained by the measurement are in accordance with the previously shown results obtained by FEM calculations for the same eccentricity level. The RMS values of the induced voltage in the measuring coils obtained by measurements due to the rotor displacement in a vertical direction are shown in the table 3. Based on these values, dependency curves between the induced voltages of the measuring coils and the rotor displacement in the vertical direction are derived. These curves are shown on the figures 10.a), 10.b) and 11. Due to the rotor displacement direction the biggest changes of the induced voltage RMS values are noticed in the measuring coils Ms1 and Ms3, as shown by the figure 10.a). Voltage changes of the coils Ms5, Ms6, Ms7 and Ms8 are also significant (figure 10.b), while voltages of measuring coils Ms2 and Ms4 had no noticeable change of RMS value (figure 11). The results obtained by the measurement are in the good alignment with the theses explained in the section with FEM results. The figure 12 shows comparison of the induced voltage in the measuring coil Ms1 obtained by FEM calculation and measurement for the case of the 25% of static eccentricity. In the case of voltage waveforms, the results are in good alignment, but some misalignment exist in the voltage amplitudes. This misalignment is the result of imperfections in coils installation, tolerances in machine design and deviations in the measurement process.

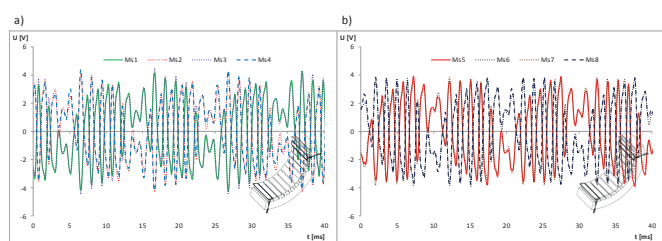


Figure 8. Measured results for the regular condition: a) induced voltage waveform in the measuring coils Ms1, Ms2, Ms3 and Ms4; b) induced voltage waveform in the measuring coils Ms5, Ms6, Ms7 and Ms8

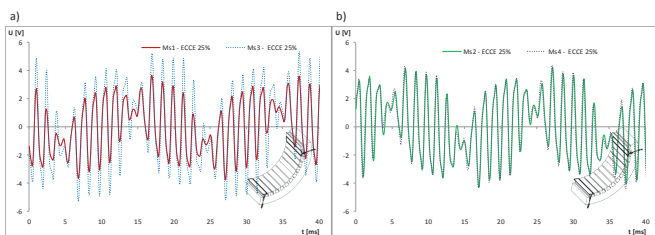


Figure 9. Measured results for the case of the 25% of static eccentricity: a) induced voltage waveform in the measuring coils Ms1 and Ms3; b) induced voltage waveform in the measuring coils Ms2 and Ms4

Table 3. RMS values of the induced voltage in the measuring coils obtained by measurements

Δ [mm]	Motion direction	MS1 [V]	MS2 [V]	MS3 [V]	MS4 [V]	MS5 [V]	MS6 [V]	MS7 [V]	MS8 [V]	MSD1 [V]	MSD2 [V]	$\Delta U_{MS1/MS3}$ [%]
-0,30	to $-y$	1,780	2,141	2,747	2,172	1,862	2,504	2,532	1,946	2,109	2,250	54,32
-0,25	to $-y$	1,819	2,133	2,638	2,166	1,895	2,44	2,461	1,973	2,116	2,234	45,02
-0,20	to $-y$	1,867	2,133	2,533	2,161	1,936	2,383	2,393	2,007	2,132	2,220	35,67
-0,15	to $-y$	1,919	2,142	2,441	2,153	1,987	2,338	2,333	2,041	2,152	2,201	27,20
-0,10	to $-y$	1,984	2,148	2,352	2,152	2,039	2,285	2,269	2,082	2,175	2,190	18,54
-0,05	to $-y$	2,045	2,148	2,268	2,151	2,095	2,240	2,210	2,126	2,181	2,170	10,90
0,00	centre	2,151	2,172	2,159	2,134	2,198	2,194	2,122	2,182	2,218	2,136	0,37
0,05	to $+y$	2,248	2,177	2,070	2,126	2,279	2,138	2,057	2,239	2,242	2,122	8,59
0,10	to $+y$	2,34	2,198	2,012	2,122	2,342	2,098	2,002	2,275	2,274	2,100	16,30
0,15	to $+y$	2,444	2,182	1,926	2,116	2,421	2,044	1,947	2,345	2,278	2,084	26,89
0,20	to $+y$	2,577	2,194	1,865	2,116	2,517	2,000	1,894	2,417	2,292	2,062	38,17
0,25	to $+y$	2,703	2,211	1,816	2,115	2,606	1,963	1,846	2,475	2,318	2,046	48,84

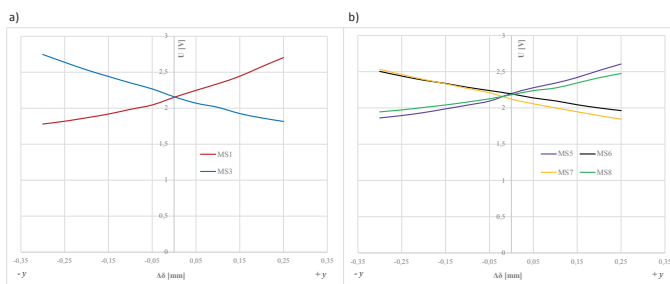


Figure 10. Changes of the induced voltage RMS values in the measuring coils due to rotor displacement in the vertical direction for different amounts of static eccentricity: a) measuring coils Ms1 and Ms3; b) measuring coils Ms5, Ms6, Ms7 and Ms8

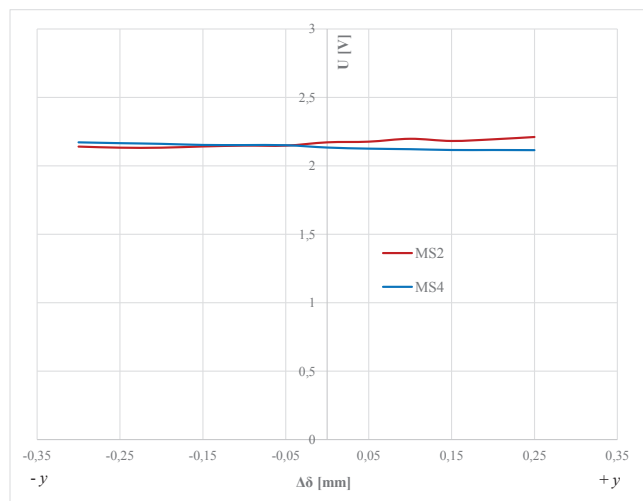


Figure 11. Changes of the induced voltage RMS values in the measuring coils due to rotor displacement in the vertical direction for different amounts of static eccentricity: measuring coils Ms2 and Ms4

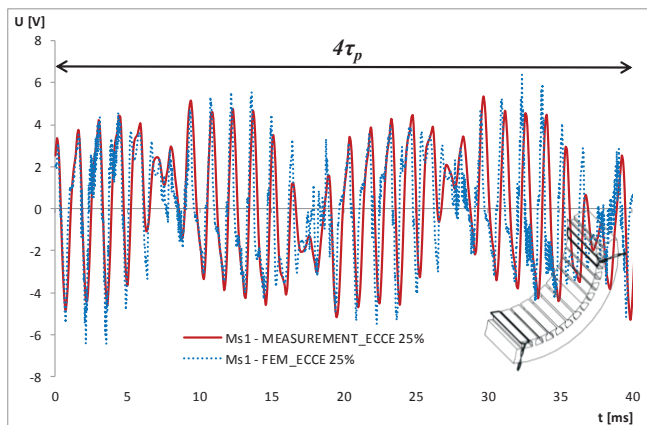


Figure 12. Comparison of the voltage induced in the measuring coil Ms1 obtained by FEM calculation and measurement for the case of the 25% of static eccentricity

CONCLUSION

The aim of this paper is a contribution to the early and reliable rotor static eccentricity detection of squirrel-cage induction machines, based on the magnetic field analysis in the air gap. The new and innovative approach for rotor static eccentricity is presented. This is patent pending solution and intellectual property of KONCAR Electrical Engineering Institute. The novelty of this new methodology is magnetic field analysis obtained by measuring coils installed in the airgap of induction machine, and spatially

spaced for pole pitch, p . By FEM calculations and measurements, it is proven that by using the measuring coils on the stator teeth it is possible to detect static eccentricity occurrence in a very early stage (practically at 10% of static eccentricity appearance). One of the main advantages of this methodology is that it avoids complex signal processing and the need for harmonic analysis of the measured signals. Determination of rotor static eccentricity is based on the changes in induced voltage waveform and RMS value of the measuring coil voltage, i.e. in the distortion of the symmetry between the induced voltage in measuring coils.

BIBLIOGRAPHY

- [1] S. Nandi, H.A. Toliyat, X. Li: »Condition Monitoring and Fault Diagnosis of Electrical Motors«, IEEE transactions on energy conversion, Vol. 20, No. 4, December 2005.
- [2] P. Tavner, L. Ran, J. Penman, H. Sedding: »Condition Monitoring of Rotating Electrical Machines«, The Institution of Engineering and Technology, London, United Kingdom, 2008.
- [3] O.V. Thorsen, M. Dalva: »A Survey of Faults on Induction Motors in Offshore Oil Industry, Petrochemical Industry, Gas Terminals, and Oil Refineries«, IEEE transactions on industry applications, Vol. 31, No.5, September/October 1995.
- [4] O.V. Thorsen, M. Dalva: »Failure Identification and Analysis for High Voltage Induction Motors in Petrochemical Industry«, IEEE, 1998.
- [5] M.L. Sin, W.L. Soong, N. Ertugrul: »Induction machine on-line monitoring and fault diagnosis – a survey«, AUPEC 2003, Australasian Universities Power Engineering Conference, Christchurch, New Zealand, October 2003. T. Seppa »Fried Wire?« (Public Utilities Fortnightly, December 2003, pages 39-41)
- [6] A. Siddique, G.S. Yadava, B. Singh: »A Review of Stator Fault Monitoring Techniques of Induction Motors«, IEEE transactions on energy conversion, Vol. 20, No. 1, March 2005. Prospec-tiva del Sector Eléctrico 2002-2011. (Secretaría de Energía, Mexico, 2002).
- [7] M.J. Picazo-Rodenas, R. Royo, J. Antonino-Daviu, J. Roger-Folch: »Use of Infrared thermography for computation of heating curves and preliminary failure detection in induction motors«, ICEM 2012, XXth International Conference on Electrical Machines, Marseille, France, September 2012.
- [8] M.E.H. Benbouzid: »A Review of Induction Motors Signature Analysis as a Medium for Faults Detection«, IEEE transactions on industrial electronics, Vol. 47, No.5, October 2000.
- [9] W.T. Thomson, R.J. Gilmore: »Motor current signature analysis to detect faults in induction drives – fundamentals, data interpretation and industrial case histories«, Proceedings of the thirty-second turbomachinery symposium, 2003.
- [10] M.Y. Kaikaa, M. Hadjami: »Effects of the Simultaneous Presence of Static Eccentricity and Broken Rotor Bars on the Stator Current of Induction Machine«, IEEE Transactions on Industrial Electronics, Vol.61, No.5, May 2014.
- [11] J. Faiz, M. Ojaghi: »Different indexes for eccentricity faults diagnosis in three-phase squirrel-cage induction motors: A review«, Elsevier, Journal of Mechatronics Vol. 19, 2009.
- [12] M. Sahraoui, A. Ghoggal, S.E. Zouzou, M.E. Benbouzid: »Dynamic eccentricity in squirrel cage induction motors – Simulation and analytical study of its spectral signatures on stator currents«, Elsevier, Simulation, Modelling, Practice and Theory, Vol. 16, August 2008.
- [13] J. Faiz, B.M. Ebrahimi, B. Akin, H.A. Toliyat: »Finite-Element Transient Analysis of Induction Motors Under Mixed Eccentricity Fault«, IEEE transactions on magnetics, Vol. 44, No. 1, January 2008.
- [14] I. Ishkova, O. Vitek: »Diagnosis of eccentricity and broken rotor bar related faults of induction motor by means of motor current signature analysis«, 16th International Scientific Conference on Electric Power Engineering (EPE), Kouty nad Desnou, Czech Republic, 20-22 May 2015.
- [15] A. Elez, J. Študír, S. Tvorčić: »Application of Differential Magnetic Field Measurement (DMFM method) in winding fault detection of AC rotating machines as part of expert monitoring systems«, CIGRE Paris 2018.